Simplex Formations of Autonomous Vehicles and Adaptive Sampling Strategies

Shahab Kalantar, Uwe Zimmer

Australian National University
Department of Information Engineering[1]

Canberra, ACT 0200, Australia
shahab.kalantar@rsise.anu.edu.au,uwe.zimmer@ieee.org

Knowledge of iso-contours of the underwater terrain can be used to reconstruct it using interpolation. Identifying a set of isoclines can be more efficient and less time-intensive than sweeping a large area. In this paper, we propose a system where a small number of agile underwater vehicles cooperatively maintain a triangular formation on a plane above the terrain and use field values measured by the individual robots to implement the simplex optimization algorithm which has proven very useful for non-smooth objective functions. In this paper, we propose general rules for implementing the reflection operation and extend it to reflexive motion over isoclines (areas of constant field value).

figure 1: Identification and tracking of isoclines.

1. Introduction

The main purpose of this paper is to explore the possibility of navigating and identifying an environment using formations of vehicles which employ an alternative mechanism for locomotion. This amounts to traversing the elements of a triangular tesselation of the plane.

Environmental exploration. A very common task for autonomous underwater multi-vehicle systems is to identify a certain set of isoclines of an ambient field (distribution). Most commonly, this field would the bottom terrain or a plume. Given this set, it would be possible to reconstruct the field in a local region [6]. Figure 1 shows a simplified senario where a vehicle (*Serafina* [1]) starts from an initial location, attempts to reach the desired isocline, while avoiding prohibited regions. In this paper, though, we employ a formation rather than a single vehicle. The main required capability is to calculate ascent (or descent) directions. Such a capability uses the values of the field at the locations of individual robots, thus obviating the need for suitable sensors. We assume that the formation is constrained to move on a horizontal plane. Given this, measuring the altitude provides the field value in the case of terrain mapping. For 3D distributions, the field is their intersection with the motion plane. Approaches based on traditional optimization strategies model the field using a quadratic approximation and try to estimate the involved parameters, i.e. gradient and Hessian (see [3], [4], [5], [7], [8], [9]). When the field is smooth enough, this task is quite straightforward and analytical formulas can be found for optimal formation shapes and sizes.

The simplex method. In real-world applications, smoothness is too big an assumption. *Zero-order* methods are a response to this. They can be classified into *derivative-free* methods, which approximate the objective function using Taylor series expansion, and direct search methods, which only require *relative ranks* of a countable set of function values. An example of the latter is the *trust-region* method. Examples of the former include simplex method, *Nelder-Mead*, and *pattern search* (which includes *compass search* and *generating-set search*). These methods are very robust and have gained much interest in the last few years due

---
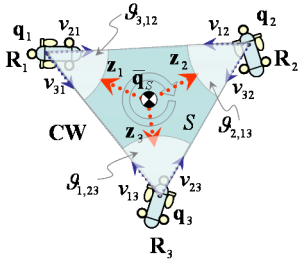
figure 2: A CW simplex formation.

figure 3: Reflective transformations.

mainly to recent theoretical developments. Refer to [10] for a good review. In this paper, we focus on the basic simplex method which uses three solutions (sensor readings by robots) to determine the worst vertex and reflect it around the opposite edge. [11] argues that this is a promising strategy for underwater applications. Recently, the authors of [12] have studied coordination strategies for this type of navigation. The main reason behind the robustness of the method is that field values are only compared and and there are only three possible actions (i.e., reflecting over an edge). Here, we propose a slightly different more general formulation and extend it to isocline tracking, in addition to the traditional hill climbing, using *minimalistic models* (line segments). Refer to [2] for a detailed description of other isocline tracking strategies employing various types of formation shapes.

Simplex formations. Consider a planar formation of three robots $\boldsymbol{R}_1$, $\boldsymbol{R}_2$ and $\boldsymbol{R}_3$ with positions $\mathbf{q}_1$, $\mathbf{q}_2$ and $\mathbf{q}_3$, measured with respect to an inertial coordinate system Υ, $\mathbf{q}_i = (x_i, y_i)^T \in \mathfrak{R}^2$. Each such formation defines a triangle $\boldsymbol{S}\{\mathbf{q}_1, \mathbf{q}_2, \mathbf{q}_3\}$ with edges $\boldsymbol{e}_{ij}$ (between $\boldsymbol{R}_i$ and $\boldsymbol{R}_j$). Note that $\boldsymbol{e}_{ij} = \boldsymbol{e}_{ji}$. If the edges are not *colinear*, the triangle defines a *simplex*. We use $\mathbf{q}_{S,i}$ to explicitly associate $\mathbf{q}_i$ with $\boldsymbol{S}$. $\boldsymbol{v}_{ij} = \mathbf{n}(\mathbf{q}_j - \mathbf{q}_i)$ is called the *edge vector*, where $\mathbf{n}(\vec{\mathbf{u}}) = \vec{\mathbf{u}}/\|\mathbf{u}\|$. Note that $\boldsymbol{v}_{ji} = -\boldsymbol{v}_{ij}$. We call $\boldsymbol{R}_k$ ($\mathbf{q}_k$) the robot (vertex) opposite $\boldsymbol{e}_{ij}$ if $k \neq i$ and $k \neq j$. Any point $\mathbf{q} \in \boldsymbol{S}$ can be expressed by

$$\mathbf{q}_w = \boldsymbol{S}(w_1, w_2, w_3) = w_1\mathbf{q}_1 + w_2\mathbf{q}_2 + w_3\mathbf{q}_3 . \qquad (1)$$

The centre of mass is given by $\bar{\mathbf{q}}_S = \boldsymbol{S}(1/3, 1/3, 1/3)$. For a point $\mathbf{q}_w \in \boldsymbol{S}$, define $z_{\mathbf{q}_w, i} = \mathbf{n}(\mathbf{q}_i - \mathbf{q}_w)$. $\boldsymbol{R}_j$ is said to be on the right (*right-hand neighbour*) of $\boldsymbol{R}_i$ (and denoted $N_r(\boldsymbol{R}_i)$) if $-z_i \times v_{ji}$ is positive ($z_i \equiv z_{\bar{\mathbf{q}}_S, i}$); otherwise, it is said to be on the left (*left-hand neighbour*) of $\boldsymbol{R}_i$ (denoted $N_l(\boldsymbol{R}_i)$). The simplex formation is called a *left-handed* (*clockwise* or *CW*) *formation* if $N_l(\boldsymbol{R}_1) = \boldsymbol{R}_2$ and $N_r(\boldsymbol{R}_1) = \boldsymbol{R}_3$. A *Right-handed* (*counter-clockwise* or C*CW*) *formation* is defined similarly. Finally, denote by $\vartheta_{i,jk}$ the angle between v_{ij} and v_{ik}, and define $L_{ij} = L_{ji} = \|\mathbf{q}_j - \mathbf{q}_i\|$. See figure 2.
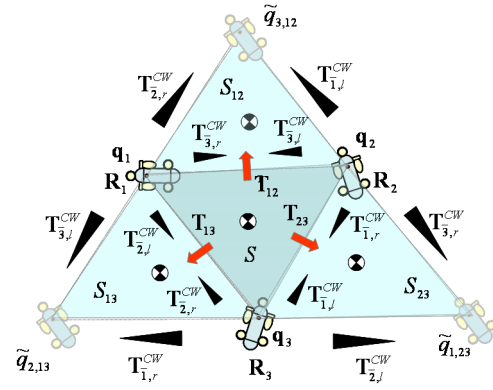
2. Motion by reflection

We use reflection as the main mechanism for locomotion. In this section, we define what we mean by reflection and discuss control rules to affect that.

Reflecting simplices. Refering to figure 3, A reflection operation on the triangle $\boldsymbol{S}$ may result in one of the three triangles $\boldsymbol{S}_{12}$, $\boldsymbol{S}_{13}$ or $\boldsymbol{S}_{23}$. $\boldsymbol{S}_{ij}$ denotes the triangle produced by reflecting $\boldsymbol{S}$ over the edge $\boldsymbol{e}_{ij}$. We say that $\boldsymbol{S}_{ij}$'s are *generated* by $\boldsymbol{S}$. A *true* reflection over $\boldsymbol{e}_{ij}$ will leave $\mathbf{q}_i$ and $\mathbf{q}_j$ untoached and will assign a new value $\mathbf{q}_{k, ij} = \mathbf{q}_i + (\mathbf{q}_j - \mathbf{q}_k)$ (or equivalently, $\mathbf{q}_j + (\mathbf{q}_i - \mathbf{q}_k)$) to $\mathbf{q}_k$. Note that this operation will reverse the sense of the triangle. Any operation assigning new values to $\mathbf{q}_1$, $\mathbf{q}_2$ and $\mathbf{q}_3$ can be represented by a matrix equation $\boldsymbol{T}\mathbf{q}_S = \mathbf{q}_S^+$, where $\mathbf{q}_S^+ = [\mathbf{q}_1^+, \mathbf{q}_2^+, \mathbf{q}_3^+]^T$ denotes the new values. $\boldsymbol{T} : \mathfrak{R}^{3 \times 2} \to \mathfrak{R}^{3 \times 2}$ is a 3 by 3 transformation matrix. Thus, true reflections over the edge $\boldsymbol{e}_{13}$, $\boldsymbol{e}_{12}$, and $\boldsymbol{e}_{23}$, producing $\boldsymbol{S}_{13}$, $\boldsymbol{S}_{12}$, and $\boldsymbol{S}_{23}$, are, respectively,

$$\boldsymbol{T}_{13} = \begin{bmatrix} \boldsymbol{e}_1^T \\ -\mathbf{1}_2^T \\ \boldsymbol{e}_3^T \end{bmatrix}, \boldsymbol{T}_{12} = \begin{bmatrix} \boldsymbol{e}_1^T \\ \boldsymbol{e}_2^T \\ -\mathbf{1}_3^T \end{bmatrix}, \boldsymbol{T}_{23} = \begin{bmatrix} -\mathbf{1}_1^T \\ \boldsymbol{e}_2^T \\ \boldsymbol{e}_3^T \end{bmatrix}. \qquad (2)$$

Here, and throughout, $\boldsymbol{e}_1$, $\boldsymbol{e}_2$ and $\boldsymbol{e}_3$ denote the standard unit base vectors for $\mathfrak{R}^3$ and $-\mathbf{1}_i$ denotes a column vector with a -1 at position i and 1 in the other positions. We use the notation $\boldsymbol{S}^+ = \boldsymbol{T}(\boldsymbol{S})$ to represent the generation of $\boldsymbol{S}^+$ under the action of $\boldsymbol{T}$ from the base triangle $\boldsymbol{S}$.

A true reflection is, of course, not a very efficient way of moving a triangle as far as a robotic formation is concerned. A more practical transition would be to keep one vertex (robot) fixed and move the other two in such a way that the sense of the triangle is preserved which also corresponds to the least amount each robot has to travel. For example, in the case shown in figure 3, to generate $\boldsymbol{S}_{13}$, we can leave $\mathbf{q}_1$ unchanged ($\mathbf{q}_1^+ = \mathbf{q}_1$), move $\mathbf{q}_2$ to $\mathbf{q}_3$ ($\mathbf{q}_2^+ = \mathbf{q}_3$) and move $\mathbf{q}_3$ to $\mathbf{q}_{2,13}$ ($\mathbf{q}_3^+ = \mathbf{q}_{2,13}$). Such a transition can be realized by $\boldsymbol{T} = \begin{bmatrix} \boldsymbol{e}_1 & \boldsymbol{e}_3 & -\mathbf{1}_2 \end{bmatrix}^T$. We call $\mathbf{q}_1$ the *pivot*, $\mathbf{q}_3$ the *leader*, and $\mathbf{q}_2$ the *follower*. We use the term "*flip-right around* $\mathbf{q}_1$" to refer to this operation.

We could have also used $\mathbf{q}_3$ as the pivot, $\mathbf{q}_1$ as the leader, and $\mathbf{q}_2$ having the same role as before. In this case, the operation will be *flipping-left around* $\mathbf{q}_3$.

To generalize, define the transformations

$$\boldsymbol{T}_{\bar{1},r}^{CW} = \begin{bmatrix} \boldsymbol{e}_1^T \\ \boldsymbol{e}_3^T \\ -\mathbf{1}_2^T \end{bmatrix}, \; \boldsymbol{T}_{\bar{1},l}^{CW} = \begin{bmatrix} \boldsymbol{e}_1^T \\ -\mathbf{1}_3^T \\ \boldsymbol{e}_2^T \end{bmatrix}, \; \boldsymbol{T}_{\bar{3},l}^{CW} = \begin{bmatrix} -\mathbf{1}_2^T \\ \boldsymbol{e}_1^T \\ \boldsymbol{e}_3^T \end{bmatrix}, \quad (3)$$

$$\boldsymbol{T}_{\bar{3},r}^{CW} = \begin{bmatrix} \boldsymbol{e}_2^T \\ -\mathbf{1}_1^T \\ \boldsymbol{e}_3^T \end{bmatrix}, \; \boldsymbol{T}_{\bar{2},r}^{CW} = \begin{bmatrix} -\mathbf{1}_3^T \\ \boldsymbol{e}_2^T \\ \boldsymbol{e}_1^T \end{bmatrix}, \; \boldsymbol{T}_{\bar{2},l}^{CW} = \begin{bmatrix} \boldsymbol{e}_3^T \\ \boldsymbol{e}_2^T \\ -\mathbf{1}_1^T \end{bmatrix}$$

Also define $\boldsymbol{T}_{\bar{i},r}^{CCW} = \boldsymbol{T}_{i,l}^{CW}$ and $\boldsymbol{T}_{\bar{i},l}^{CCW} = \boldsymbol{T}_{i,r}^{CW}$, for $i \in \{1, 2, 3\}$. Note that $\boldsymbol{T}_{\bar{1},r}^{CW}$, $\boldsymbol{T}_{\bar{3},l}^{CW}$ (in the clock-wise case) and $\boldsymbol{T}_{\bar{2},l}^{CCW}$ and $\boldsymbol{T}_{\bar{1},r}^{CCW}$ (in the counter-clock-wise case) produce the same triangle $\boldsymbol{S}\{\mathbf{q}_1, \mathbf{q}_2, \mathbf{q}_{2,13}\}$, and similarly for the other cases and transformations. Let τ_S denote the sense of the formation: it is 1 if the sense is CW and 0 otherwise. Let λ_i denote the desired direction of flipping around the pivot $\mathbf{q}_i$: it is 1 if left flipping is desired and -1 otherwise. Now, a transformation around a pivot $\mathbf{q}_i$ can in general be represented by the expression

$$\boldsymbol{T}_i = (\lambda_i \boldsymbol{T}_{i,l}^{CW} + \bar{\lambda}_i \boldsymbol{T}_{i,r}^{CW}) + \tau_S (\lambda_i \boldsymbol{T}_{i,l}^{CCW} + \bar{\lambda}_i \boldsymbol{T}_{i,r}^{CCW}). \quad (4)$$

After rearranging, we get

$$\boldsymbol{T}_i = (\lambda_i + \tau_S \bar{\lambda}_i) \boldsymbol{T}_{i,l}^{CW} + (\bar{\lambda}_i + \tau_S \lambda_i) \boldsymbol{T}_{i,r}^{CW}. \quad (5)$$

Here, $\bar{\lambda}_i = 1 - \lambda_i$. Let β_i denote a variable which determines if $\mathbf{q}_i$ is the pivot or not, taking its values in $\{0, 1\}$, and such that $\beta_1 + \beta_2 + \beta_3 = 1$. Note that λ_i is defined only when $\beta_i = 1$. Now, the transformation taking a triangle $\boldsymbol{S}$ to its new state $\boldsymbol{S}^+$ is given by

$$\boldsymbol{T} = \beta_1 \boldsymbol{T}_1 + \beta_2 \boldsymbol{T}_2 + \beta_3 \boldsymbol{T}_3. \quad (6)$$

In the remainder, we will make things simpler by fixing the sense of the formation at CW, thus dealing with the simplified matrix

$$\boldsymbol{T} = \beta_1 (\lambda_1 \boldsymbol{T}_{\bar{1},l}^{CW} + \bar{\lambda}_1 \boldsymbol{T}_{\bar{1},l}^{CW}) + \quad (7)$$
$$\beta_2 (\lambda_2 \boldsymbol{T}_{\bar{2},l}^{CW} + \bar{\lambda}_2 \boldsymbol{T}_{\bar{2},l}^{CW}) + \beta_3 (\lambda_3 \boldsymbol{T}_{\bar{3},l}^{CW} + \bar{\lambda}_3 \boldsymbol{T}_{\bar{3},l}^{CW})$$

If $\boldsymbol{S}(t)$ represents a formation at a particular time, a planning scheme should determine the pivot robot $\boldsymbol{R}_i$ (meaning, $\beta_i = 1$ and $\beta_j = 0$ for $j \neq i$) and λ_i, depending on the application. The control law should then guide the robots to the new state $\boldsymbol{T}(\boldsymbol{S}(t))$ giving $\boldsymbol{S}(t + \Delta t)$ where Δt is the time taken to reconfigure the formation.

Note that, due to linearity of $\boldsymbol{T}$, nothing changes if relative coordinates with respect to any point within the triangle is used.

It is often useful to regard the sequence of reflections, as determined by a planning scheme, as a *discrete process*. Lets imagine that we have a formation determined by the triangle $\boldsymbol{S}$ at some initial time. We denote this triangle by $\boldsymbol{S}[0]$. $\boldsymbol{S}^+ = \boldsymbol{T}(\boldsymbol{S}[0])$ is then denoted by $\boldsymbol{S}[1]$ and so on. Thus, the output of a planning module can be regarded as the generation of a sequence $\boldsymbol{S}[k]$, according to some goal. We call k a step. For instance, in the problem of lo-

calizing the source of a plume, the sequence should converge to a position on the plane which corresponds to a maximum value of the plume, in the sense that there should be a $\bar{k}$ such that for $k \geq \bar{k}$, we have $\|\bar{\mathbf{q}}_{S[k]} - \mathbf{q}_*\| \leq \varepsilon$ where $\mathbf{q}_* \in \mathfrak{R}^2$ and $\mathbf{f}(\mathbf{q}_*)$ is an extremum of the plume distribution $\mathbf{f}: \mathfrak{R}^2 \to \mathfrak{R}$. To be consistent, all the variables $\boldsymbol{x}$ associated with step k also have the alternate representation $\boldsymbol{x}[k]$. $\boldsymbol{x}[k]$ represents the value of $\boldsymbol{x}$ just before transition, $\boldsymbol{x}(t)$ is its value during transition, and $\boldsymbol{x}[k + 1]$ the value just after the completion of transition. This is most beneficial when the time it takes to transform or the current time is not relevant to the problem at hand.

Control rules. Given a triangular formation with underlying triangle $\boldsymbol{S}\{\mathbf{q}_1, \mathbf{q}_2, \mathbf{q}_3\}$, we want to design control laws to drive the vertex robots to their new positions as determined by transformation $\boldsymbol{T}$. In an idealized world, the simplest form of such a control law, assuming that global inertial positions are known by each robot, is given by

$$\dot{\mathbf{q}}(t) = k(\boldsymbol{T}\mathbf{q}(t_0) - \mathbf{q}(t)), \quad (8)$$

where t_0 is the time the motion is started and k is an appropriate gain. At a final time $t_f = t_0 + \Delta t$, the robots would hopefully be at their destination, i.e., $\boldsymbol{q}(t_f) = \boldsymbol{T}\boldsymbol{q}(t_0)$. In practice, though, dependence on global positioning knowledge is outruled and positioning is not perfect. Note that a general triangular formation changes its shape under the reflection operation and hence cannot be treated as a rigid formation; the reflected shape cannot be obtained by only translation of $\bar{\mathbf{q}}_S$ and rotation around it. The leader-follower scheme provides a reasonable solution. Denote by $\boldsymbol{R}_p$, $\boldsymbol{R}_l$ and $\boldsymbol{R}_f$, the pivot, leader and follower robots. Suppose that the robots have one of the roles at all times. Initially, the roles can be assigned arbitrarily. We can regard $\boldsymbol{R}_p$ as the leader in the leader-follower scheme and $\boldsymbol{R}_l$ and $\boldsymbol{R}_f$ as followers. Fix local coordinate frame Υ_i on $\boldsymbol{R}_i$ which is aligned with the compass direction; for example, y_{Υ_i} is aligned with the north and x_{Υ_i} points to the east. This implies that robots are equipped with compass modules. Since the frames have the same orientation, we may simply use $\mathbf{q}_{ij} = \mathbf{q}_j - \mathbf{q}_i$ to represent the position of $\boldsymbol{R}_j$ relative to the frame attached to $\boldsymbol{R}_i$. This relative position can also be represented by the distance-bearing pair (L_{ij}, ϑ_{ij}). The bearing is with respect to the x axis. Knowledge of distances (L_{pf}, L_{pl}, L_{fl}) and ϑ_{pf} is sufficient for representing, uniquely, the state of the simplex. Alternatively, we could use L_{pf}, L_{pl}, ϑ_{pf}, and $\vartheta_{p,fl}$. The pivot tries to keep station and the other two try to maintain the desired values L_{pf}^d, L_{pl}^d, L_{fl}^d, ϑ_{pf}^d, $\vartheta_{p,fl}^d$ for the above parameters. This implies that the robots are capable of measuring distances and bearings. If new roles are assigned to the robots, new desired values can be easily computed (we skip the formulas here). Starting with $k = 1$ and assuming that the actual values of the parameters are sufficiently close to desired ones, $\boldsymbol{S}[k + 1]$ can be computed by applying $\boldsymbol{T}$ to $(\mathbf{0}_3, \mathbf{q}_{pf}^d, \mathbf{q}_{pl}^d)$. Note the important fact that the desired values are not calculated based on any measured values but are computed based on those of
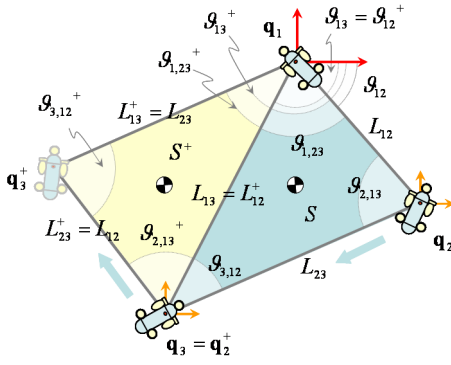
figure 4: Reflection.

the previous iteration. Using measured values has the serious problem that the transformation is not *exact* in the sense that $S[k+1]$ may not be exactly $T(S[k])$, even if $\lVert x[k+1] - x^+[k] \rVert \le \delta$ for very small δ. If decision about subsequent motions of the formation is solely based on the current actual state of the formation, the errors can lead to considerable *drift* causing future states to diverge away from their *initial shape*. This initial shape is characterized by size and aspect ratio rather than geometrical relationships between individual robots which may, of course, change from one state to the other. Suitable control laws determine evolution equations for relative ranges and bearings between individual robots based on the errors $L_{p\alpha}(t) - L_{p\alpha}^d[k+1]$, $\vartheta_{p\alpha}(t) - \vartheta_{p\alpha}^d[k+1]$, etc. These laws should be translated to equations prescribing linear and angular velocities for individual robots. Finally, although there is, in theory, no need for any interaction between the follower and the leader, providing such a coupling will increase robustness and safety in practice. Figure 4 demonstrates reflection.

3. Reaching isoclines

The formation would start from an initial position relatively close to some desired isocline. Depending on the value of the isocline and the value of the field at the current position, the formation needs to climb uphill or downhill to reach the isocline.

Finding extrema. In the simplest simplex method, optima of a real valued function $\mathbf{f}: \mathfrak{R}^2 \to \mathfrak{R}$ are sought by comparing function values $\mathbf{f}(\mathbf{q}_i(t))$ at the three vertices of the triangle. The *worst* vertex, i.e., the one which has the largest (smallest) value is discarded and replaced with a new vertex which hopefully has the smallest (largest) value among the three vertices. Thus, a new triangle is formed and search is continued. When the goal is to find the maximum of the field, the worst vertex (denoted $\mathbf{q}_W$) corresponds to the smallest value, the *best* vertex (denoted $\mathbf{q}_B$) has the largest value and the *next worst* vertex (denoted $\mathbf{q}_{NW}$, or $\mathbf{q}_{NB}$) is such that $\mathbf{f}(\mathbf{q}_W) \le \mathbf{f}(\mathbf{q}_{NW}) \le \mathbf{f}(\mathbf{q}_B)$. In case of equality, the ordering can be random or according to some other default rule. When finding minima, the ordering is reversed. Now, $\mathbf{q}_W$ is replaced by a vertex construct-

ed by reflecting $\mathbf{q}_W$ through the middle point $\mathbf{M} = (\mathbf{q}_B + \mathbf{q}_{NB})/2$ of the edge connecting $\mathbf{q}_B$ and $\mathbf{q}_{NB}$. The rationale is that the function value decreases (increases) along the edge of the triangle connecting $\mathbf{q}_W$ and $\mathbf{q}_B$ and also along the edge connecting $\mathbf{q}_W$ to $\mathbf{q}_{NB}$. It may now be the case that the function takes smaller (larger) values in the area away from $\mathbf{q}_W$ on the opposite side of $\overline{\mathbf{q}_B \mathbf{q}_{NB}}$. The expression for the new vertex (also called the *test point*) would thus be

$$\mathbf{q}_W^+ = \mathbf{M} + (\mathbf{M} - \mathbf{q}_W). \tag{9}$$

When finding optima, a common stopping criterion is test for *flatness*: a triangle is flat if function values at the vertices are approximately the same. More formally, the process of generation of triangles stops whenever

$$\left(\frac{1}{3} \sum_{i=1}^{3} (\mathbf{f}(\mathbf{q}_i) - \bar{\mathbf{f}}) \right)^{1/2} < \delta, \tag{10}$$

for some prespecified δ.

Let ρ be 1 if the formation should go down hill, determined by the conditions $\mathbf{f}(\mathbf{q}_1) > \mathbf{c}_d$, $\mathbf{f}(\mathbf{q}_2) > \mathbf{c}_d$, $\mathbf{f}(\mathbf{q}_3) > \mathbf{c}_d$, and 0 if the conditions $\mathbf{f}(\mathbf{q}_1) < \mathbf{c}_d$, $\mathbf{f}(\mathbf{q}_2) < \mathbf{c}_d$ and $\mathbf{f}(\mathbf{q}_3) < \mathbf{c}_d$ are satisfied. In the first case, we have

$$\mathbf{f}(\mathbf{q}_W) > \max\{\mathbf{f}(\mathbf{q}_{N_l(\mathbf{R}_W)}), \mathbf{f}(\mathbf{q}_{N_r(\mathbf{R}_W)})\}, \tag{11}$$

and in the second case

$$\mathbf{f}(\mathbf{q}_W) < \min\{\mathbf{f}(\mathbf{q}_{N_l(\mathbf{R}_W)}), \mathbf{f}(\mathbf{q}_{N_r(\mathbf{R}_W)})\}. \tag{12}$$

Either of $\mathbf{q}_B$ or $\mathbf{q}_{NB}$ can be chosen as the pivot. By default, we select the vertex to the left of $\mathbf{q}_W$ as the pivot, the one to the right as the leader and $\mathbf{R}_W$ as the follower. Thus, we simply set $\beta_{N_l(\mathbf{R}_W)} = 1$, and $\lambda = 1$ for left rotation. Denote by $\mathbf{f}_{i,jk}$ the boolean variable which is true if $\mathbf{f}(\mathbf{q}_i) > \max\{\mathbf{f}(\mathbf{q}_j), \mathbf{f}(\mathbf{q}_k)\}$ and by $\mathbf{f}_{i,jk}$ the condition that $\mathbf{f}(\mathbf{q}_i) < \min\{\mathbf{f}(\mathbf{q}_j), \mathbf{f}(\mathbf{q}_k)\}$. Now, define

$$\beta_1 = (\rho \wedge \mathbf{f}_{3,12}) \vee (\bar{\rho} \wedge \mathbf{f}_{3,12}), \tag{13}$$

$$\beta_2 = (\rho \wedge \mathbf{f}_{1,23}) \vee (\bar{\rho} \wedge \mathbf{f}_{1,23}), \tag{14}$$

$$\beta_3 = (\rho \wedge \mathbf{f}_{2,13}) \vee (\bar{\rho} \wedge \mathbf{f}_{2,13}). \tag{15}$$

If $\beta_1 = 1$, we have $\mathbf{R}_l = \mathbf{R}_2$, $\mathbf{R}_f = \mathbf{R}_3$. The other cases are treated similarly.

Contact with isoclines. It is a well-known fact that this simple strategy can run into difficulties, especially when close to optima. Here, we are only interested in placing the formation on the desired isocline rather than finding optima and we assume that the formation is relatively close to it. As soon as the formation touches the desired isocline, the control regime may change to that of isoline traversal, as described later. Overlapping of the formation with the isoline occurs if the straight line representing the isoline in the linear interpolation of the field (see section 4) crosses the triangle. If this line is well inside the triangle, then the formation can proceed to isoline traversal. If it is only touching the triangle, then we have to decide on which re-

figure 5: Possible cases when the formation gets into contact with an isocline.
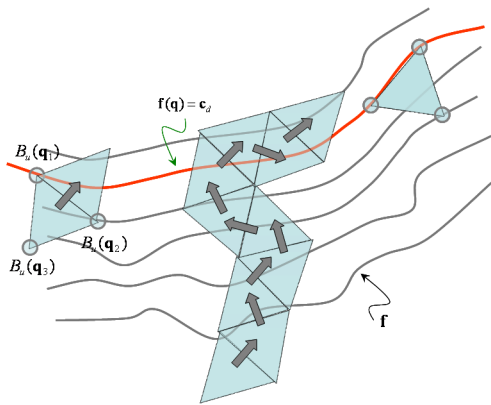
figure 6: Linear interpolation of the field.

gime to switch to. It makes sense to consider the boundary of the triangle, denoted ∂S and composed of the vertices and the edges (sides), as an *uncertain* region. Let w_1 and w_2 be the intersections of the interpolated isoline with ∂S. We define *uncertainty regions* $\boldsymbol{B}_u(q_i)$ around the vertices as balls (circles) with some user-defined radius δ_u. The line $L\{w_1, w_2\}$ is said to be touching ∂S if $w_1 \in \boldsymbol{B}_u(q_i)$ and $w_2 \in \boldsymbol{B}_u(q_j)$ for some i and j. If $i \neq j$, L lies on the edge $\boldsymbol{e}_{ij}$. Otherwise, L is only touching one vertex. See figure 5 for illustration. The former case is considered *unambiguous* since the orientation of the line is completely known. This case can be handled by translating the formation in the direction perpendicular to the isocline (see section 5). The latter case presents some ambiguity as the line is only touching one vertex and its orientation can not be determined. In this case, it is safer to continue climbing until an unambiguous situation is reached. In normal operating conditions, the formation starts from some place inside or outside the closed curve defining the isoline. Upon reaching the isoline, traversal on the isoline commences. While on the isoline, if the curvature is too high, reflection of the triangle can cause the formation to fall outside the isoline. This event signals switching to climbing behaviour. One serious drawback of this simple scheme is that if the triangle is on a *saddle point*, two consecutive reflections may return the triangle to the same spot. We assume that, in face of uncertainties, this condition rarely occurs.

4. Tracking isoclines

To be able to follow an isocline, the formation has to first generate a model for the distribution. In this section, we propose linear interpolation for this purpose and define the required transformations.

Linear interpolation. Let a field $\mathbf{f}:\Omega \to \Re$ be given. Consider a formation with triangle $\boldsymbol{S}\{\mathbf{q}_1, \mathbf{q}_2, \mathbf{q}_3\}$. Let $v(\mathbf{q}) = a_{00} + a_{10}x + a_{01}y$. The degrees of freedom for $\boldsymbol{S}$
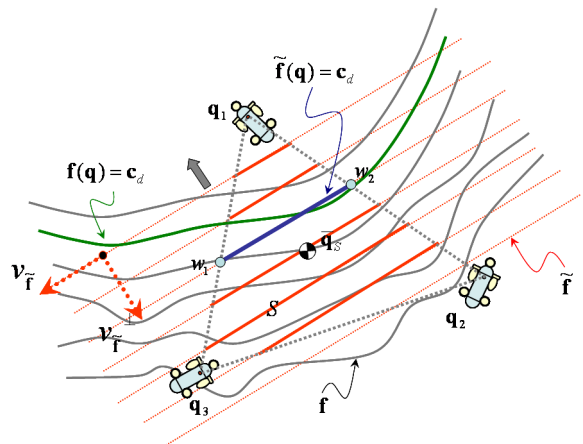
are $\mathbf{f}(\mathbf{q}_S) = [\mathbf{f}(\mathbf{q}_1), \mathbf{f}(\mathbf{q}_2), \mathbf{f}(\mathbf{q}_3)]^T$. We should have $v(\mathbf{q}_i) = \mathbf{f}(\mathbf{q}_i)$ which gives the linear system

$$\mathbf{f}(\mathbf{q}_S) = \mathbf{1}_3 \mathbf{a}^T \begin{bmatrix} 1 & 1 & 1 \\ \mathbf{q}_1 & \mathbf{q}_2 & \mathbf{q}_3 \end{bmatrix}, \qquad (16)$$

where $\mathbf{a} = [a_{00}, a_{10}, a_{01}]^T$. This system has a unique solution if $|\boldsymbol{B}| \neq 0$ where

$$\boldsymbol{B} = \begin{bmatrix} \mathbf{q}_1^T & 1 \\ \mathbf{q}_2^T & 1 \\ \mathbf{q}_3^T & 1 \end{bmatrix}. \qquad (17)$$

But, $|\boldsymbol{B}| = \mathbf{L}_S^2 \sin(\pi/3)$ (the area of $\boldsymbol{S}$, where $\mathbf{L}$ is the side length) which implies that $\boldsymbol{B}$ is non-singular. This means that a linear function v can be uniquely determined by the values of the field at the vertices. This unique solution is given by

$$\mathbf{a} = \frac{1}{\Delta} \begin{bmatrix} |\mathbf{A}_1| & |\mathbf{A}_2| & |\mathbf{A}_3| \\ (\mathbf{q}_2 - \mathbf{q}_3)^\perp & (\mathbf{q}_3 - \mathbf{q}_1)^\perp & (\mathbf{q}_1 - \mathbf{q}_2)^\perp \end{bmatrix} \mathbf{f}(\mathbf{q}), \qquad (18)$$

$$\Delta = |\mathbf{A}_1| + |\mathbf{A}_2| + |\mathbf{A}_3|, \qquad (19)$$

$$\mathbf{A}_1 = \begin{bmatrix} \mathbf{q}_2^T \\ \mathbf{q}_3^T \end{bmatrix}, \ \mathbf{A}_2 = \begin{bmatrix} \mathbf{q}_3^T \\ \mathbf{q}_1^T \end{bmatrix}, \ \mathbf{A}_3 = \begin{bmatrix} \mathbf{q}_1^T \\ \mathbf{q}_2^T \end{bmatrix}. \qquad (20)$$

The procedure outlined above defines a mapping $\Psi^I : \Re^{3 \times 2} \times \Re^3 \to \Re^3$, $\mathbf{a} = \Psi^I(\mathbf{q}, \mathbf{f}(\mathbf{q}_S))$.

We use the notation $\tilde{\mathbf{f}}(\mathbf{q}_S)$ instead of $v(\mathbf{q})$. $\tilde{\mathbf{f}}(\mathbf{q}_S)$ is a bi-linear polynomial approximation of $\mathbf{f}(\mathbf{q})$. The contour lines of $\tilde{\mathbf{f}}$ are straight lines with slope $m_{\tilde{\mathbf{f}}} = -a_{10}/a_{01}$ (figure 6). If the triangulation is fine enough, $\tilde{\mathbf{f}}$ can be a good approximation of $\mathbf{f}$. In terms of formations, this translates to having smaller formation sizes. If we put $\theta_{\tilde{\mathbf{f}}} = \text{atan}(m_{\tilde{\mathbf{f}}})$, then $v_{\tilde{\mathbf{f}}} = (\cos(\theta_{\tilde{\mathbf{f}}}), \sin(\theta_{\tilde{\mathbf{f}}}))^T$ gives the vector tangent to the lines and $\text{perp}(v_{\tilde{\mathbf{f}}})$ is the vector perpendicular (normal) to them, pointing in the direction of the minimum.

Intersection with isoclines. In the linear model, the contour approximating the isoline is given by $\mathbf{f}(\mathbf{q}) = \mathbf{c}_d$. The intersection of this line with an edge $\{\mathbf{q}_i, \mathbf{q}_j\}$ is given by

$$w_{ij} = \frac{1}{\begin{bmatrix} a_{10} & a_{01} \end{bmatrix} \cdot (\mathbf{q}_j - \mathbf{q}_i)} ((a_{00} - \mathbf{c}_d)(q_i - q_j) + \qquad (21)$$

$$\begin{bmatrix} a_{01} & a_{10} \end{bmatrix} \cdot \begin{bmatrix} |\boldsymbol{Q}_1| & |\boldsymbol{Q}_2| \end{bmatrix})$$

$$\boldsymbol{Q}_1 = \begin{bmatrix} \mathbf{q}_i & \mathbf{q}_i \end{bmatrix}^T, \boldsymbol{Q}_2 = \begin{bmatrix} \mathbf{q}_j & \mathbf{q}_i \end{bmatrix}. \qquad (22)$$

Only two of the three points w_{12}, w_{13} and w_{23} correspond to intersections with the triangle. w_{ij} has to be checked to see if it lies on the line connecting $\mathbf{q}_i$ and $\mathbf{q}_j$ and that it is within the segment $\{\mathbf{q}_i, \mathbf{q}_j\}$. Thus, w_{ij} is an intersection if

$$\frac{|(\mathbf{q}_j - \mathbf{q}_i) \times (\mathbf{q}_i - w_{ij})|}{\|\mathbf{q}_j - \mathbf{q}_i\|} = 0, \qquad (23)$$

$(\mathbf{q}_j - \mathbf{q}_i) \cdot (w_{ij} - \mathbf{q}_i) \geq 0$ and $\|w_{ij} - \mathbf{q}_i\| \leq \|\mathbf{q}_j - \mathbf{q}_i\|$. If $w_{\alpha_1 \beta_1}$ and $w_{\alpha_2 \beta_2}$ satisfy these, they are denoted as w_1 and w_2. We denote by $\Psi_I^w : \Re^{3 \times 2} \times \Re^3 \times \Re \to \Re^2 \times \Re^2$ the mapping which produces (w_1, w_2) given $(\mathbf{q}_1, \mathbf{q}_2, \mathbf{q}_3, (a_{00}, a_{01}, a_{10}), \mathbf{c}_d)$. We define $\Psi^w = \Psi_I^{w} \circ \Psi^I$. If the size of the triangle is sufficiently small, the procedure outlined above is valid only in a small neighborhood around the triangle. As we go farther from the triangle, the linear model diverges from the true isoline, especially in areas with high curvatures. It is a well-known fact that this interpolation is continuous across the common boundary between touching triangles. The same statement is generally not true for $\partial \mathbf{f}/\partial \mathbf{q}$. The scheme described above is the basis of many contouring algorithms [13].

Reflection over isoclines. Let $\gamma_d : \Re \to \Re^2$ denote the closed curve (isoline) of the field $\mathbf{f}$, induced by the desired field value $\mathbf{c}_d$, parametrized by $s \in \Re$. By definition, flipping under T moves the formation *left* if

$$\gamma_d^{-1}(Q(\bar{\mathbf{q}}s, \gamma_d)) < \gamma_d^{-1}(Q(\bar{\mathbf{q}}_{T(s)}, \gamma_d)). \qquad (24)$$

Moving *right* is similarly defined. Q is the closest point operator. The sense will be preserved (the formation will always be moving left or right) if the region enclosed by γ_d always has field values either greater or smaller than the region outside it. This is, of course, an abstraction but states what the ideal situation can be.

If such a condition applies, then flipping rules on the isoline can be un-ambiguously defined. Let us denote by $\boldsymbol{L}_{i,jk}^w$ the boolean variable which is true if $\{w_1, w_2\}$ intersects the edge $\{\mathbf{q}_j, \mathbf{q}_k\}$. We set

$$\beta_1 = \sigma_0(\boldsymbol{L}_{1,23}^w \wedge (\mathbf{f}_{1,23} \vee \mathbf{f}_{1,23})), \qquad (25)$$

$$\beta_2 = \sigma_0(\boldsymbol{L}_{2,13}^w \wedge (\mathbf{f}_{2,13} \vee \mathbf{f}_{2,13})), \qquad (26)$$

$$\beta_3 = \sigma_0(\boldsymbol{L}_{3,12}^w \wedge (\mathbf{f}_{3,12} \vee \mathbf{f}_{3,12})), \qquad (27)$$

where $\sigma_0(u)$ is 1 if u is true, and 0 otherwise. Only one of β_1, β_2 or β_3 is true at any time. The direction of flipping is determined by the formula
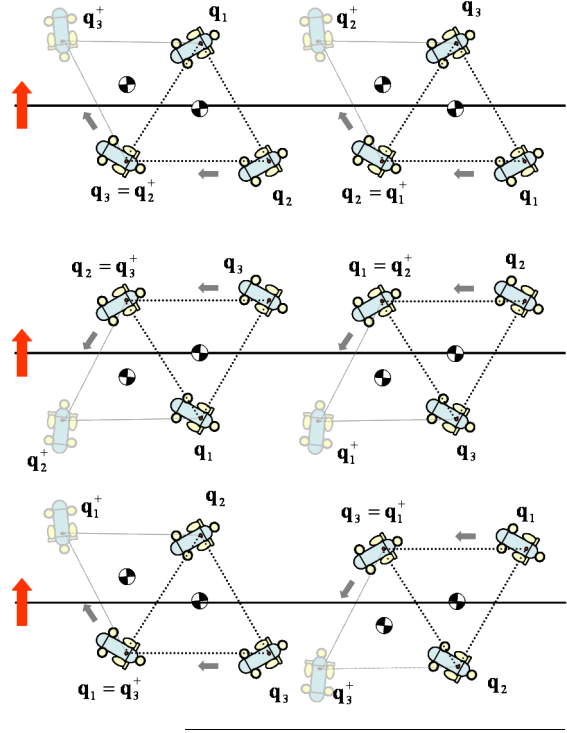
figure 7: All the possible transformations of simplices over an isoline.

$$\lambda = \tilde{d} \sigma_{-1}(\mathbf{f}_{p, N_l(\boldsymbol{R}_p)N_r(\boldsymbol{R}_p)}, \mathbf{\bar{f}}_{p, N_l(\boldsymbol{R}_p)N_r(\boldsymbol{R}_p)}), \qquad (28)$$

where $\sigma_{-1}(u_1, u_2)$ is -1 if u_1 is true, and 1 if u_2 is true. It is undefined if both u_1 and u_2 are false. p (the index of the pivot vehicle) is such that β_p is true. d is a user-defined direction of traversal. It should be 1 for left and -1 for right. Figure 7 shows all the possible situations for a clockwise formation with $d = 1$. In the figure, the thick black lines represent the isoline and the red arrows show the direction of increase of the field.

5. Other considerations

In this section, we will mention some of the issues that are important ingredients of a complete system but which we will defer their discuss in detail to future publications.

Location adjustment. As was mentioned previously, as contact between the interpolated isocline and the triangle approaches the vertices or sides, uncertainty regarding reflection increases. To address this, we can associate circular *critical regions* $\boldsymbol{B}_c(\mathbf{q}_i)$ with vertices. It is preferable that $L\{w_1, w_2\}$ lie in the *safe region* (the area of the triangle minus the critical regions) and be as close to passing through $\bar{\mathbf{q}}_S$ as possible. To do this, after each reflection, we should translate and rotate the formation appropriately. This is the only departure from the main reflective motion.

Size adjustment. To decrease interpolation error, the size of the formation should change in accordance with the lo-

cal curvature of the field. Rather than trying to compute an optimal size, based on direct curvature estimates (which may not be practical), we may accumulate evidence E which indirectly hints at the local curvature and interpret it as some sort of potential energy. The difference $E_e = E_t - E$ can then be used as a *force* acting on the formation, where E_t is a predefined tolerance threshold. As the curvature (energy) increases, the formation should be *forced* to shrink and as it decreases, the formation can relax back to a given nominal size, A_n, for faster traversal.

Station keeping. One particular use of a linear model (or any model, for that matter), is to enable a formation to keep station at a fixed position with respect to a field, once an isocline has been reached. The obvious strategy of using flowmeters on vehicles to counteract ambient flow can be further enhanced by also moving the formation in the direction defined by $v_{\bar{\mathbf{f}}}^{\perp}$. This will keep the formation on a desired isocline if disturbances are sufficiently small. The shortcoming of this approach is that isoclines are radially defined. In other words, the formation may, under external disturbances, move along the isocline without even noticing it. If the field is anything other than the natural bottom terrain, then a *fusion* of the two linear models corresponding to these fields can be used to make station keeping more robust. We may, for example, use the motion law

$$\dot{\bar{\mathbf{q}}}s = \beta_1(\bar{\mathbf{e}} - \bar{\mathbf{e}}_0)v_{\bar{\mathbf{e}}}^{\perp} + \beta_2(\bar{\mathbf{f}} - \bar{\mathbf{f}}_0)\langle v_{\bar{\mathbf{f}}}^{\perp}, v_{\bar{\mathbf{e}}}\rangle v_{\bar{\mathbf{e}}} \qquad (29)$$

for the centre of mass of the formation, where $\mathbf{e}$ denotes the field defined by the terrain, t_0 denotes the time instant when the reference isoclines were computed, and $\bar{\mathbf{e}}$ and $\bar{\mathbf{f}}$ denote average field values of the robots, $\bar{\mathbf{f}}_0 = \bar{\mathbf{f}}(t_0)$, $\bar{\mathbf{e}}_0 = \bar{\mathbf{e}}(t_0)$. This is, of course, only effective if the two models are not co-linear.

Reflection by rotation. Irregular triangular elements have the benefit that they can become highly stretched along regions of rapid variations. In this paper, we only considered regular triangles where reflection can be done by just rotation around the pivot. In a regular triangle,

$$L_{12} = L_{13} = L_{23} = L_d = \left(\frac{2A_d}{\sin(\pi/3)}\right)^{1/2}, \qquad (30)$$

$$\vartheta_{3,12} = \vartheta_{1,23} = \vartheta_{2,13} = \frac{\pi}{3}, \qquad (31)$$

where A_d is a desired size (area) for the triangle. We then have

$$\vartheta_{pf}^d[k] = \vartheta_{pf}^d[k-1] + \lambda(\pi/3), \qquad (32)$$

$$\vartheta_{pl}^d[k] = \vartheta_{pf}^d[k-1] + \lambda(2\pi/3). \qquad (33)$$

Cooperative formations. In practice, it may take a long time for a single triangular formation to identify all the isoclines of interest in a region. Moreover, if global positioning is not an option, a single formation cannot even determine if it has finished tracking the whole length of an
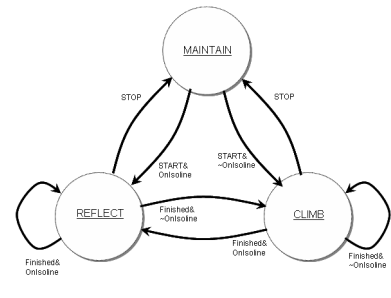
figure 8: Operation state diagram.

isocline. It seems reasonable to imagine the deployment of several (identical) formations. For example, two formations can start from positions close to each other and close to an isocline and track it in opposite directions. They have to meet each other at the other end after a finite time. Then, they can consider climbing together uphill (or downhill) to a differnt isocline and do the same thing again. In a more advanced senario, a large group of simplex formations may be scattered throughout a region to speed up the mission. During the mission, the space two or more formations may overlap to the extent that they may come into contact with each other. This requires the provision of mechanisms to prevent collisions.

Obstacle avoidance. The method proposed for moving on an isocline using reflexive motion can also be used for negotiating obstacles. Suppose that an obstacle can be represented with a possibly non-convex curve γ_{O}. We can use a distance function $D_{\mathbf{O}}: \mathfrak{R}^2 \to \mathfrak{R}$ to create an artificial potential around the obstacle. Let $U_{\mathrm{O}}: \mathfrak{R}^2 - (\mathrm{Int}(\gamma_{\mathrm{O}}) \cup \gamma_{\mathrm{O}}) \to [0, 1]$ denote this potential. $U_{\mathrm{O}}(\mathbf{q}) \to 1$ as $D(\mathbf{q}, \gamma_{\mathrm{O}}) = \|\mathbf{q} - Q(\mathbf{q}, \gamma_{\mathrm{O}})\| \to 0$, and $U_{\mathrm{O}}(\mathbf{q}) \to 0$ as $D(\mathbf{q}, \gamma_{\mathrm{O}}) \to \infty$. Consider the isocline of this artificial field defined by $U_{\mathrm{O}}(\mathbf{q}) = u_0$ and denote it γ_0. This isocline can also be defined as the curve with *safe* distance d_0 from γ_{O}. Let the sensing range of the vehicles be r and assume, for simplicity, that r is sufficiently greater than d_0. Also assume that the obstacle is sufficiently far from the desired field isocline. Fix an arbitrary direction for traversal of the obstacle isocline. In the absence of any othet field, the formation can traverse along γ_0 in this direction.

Now suppose that the formation is climbing uphill to reach the isocline. If all the vehicles in the formation can sense the obstacle, the obstacle field U_{O} is interpolated along with the target field. If the current simplex overlaps with γ_0, two possible cases may arise. Either the reflexive actions for climbing and that for tracking γ_0 are the same or they are conflicting. If they are the same, the action is executed. Note that of the three possible reflections, two are on the obstacle isoline and one is either away from this isocline or else it is towards the interior of it. If the action required by climbing is the one away from the obstacle, it means that the obstacle is no longer on the path to field isocline and we can safely ignore the obstacle field. If this is
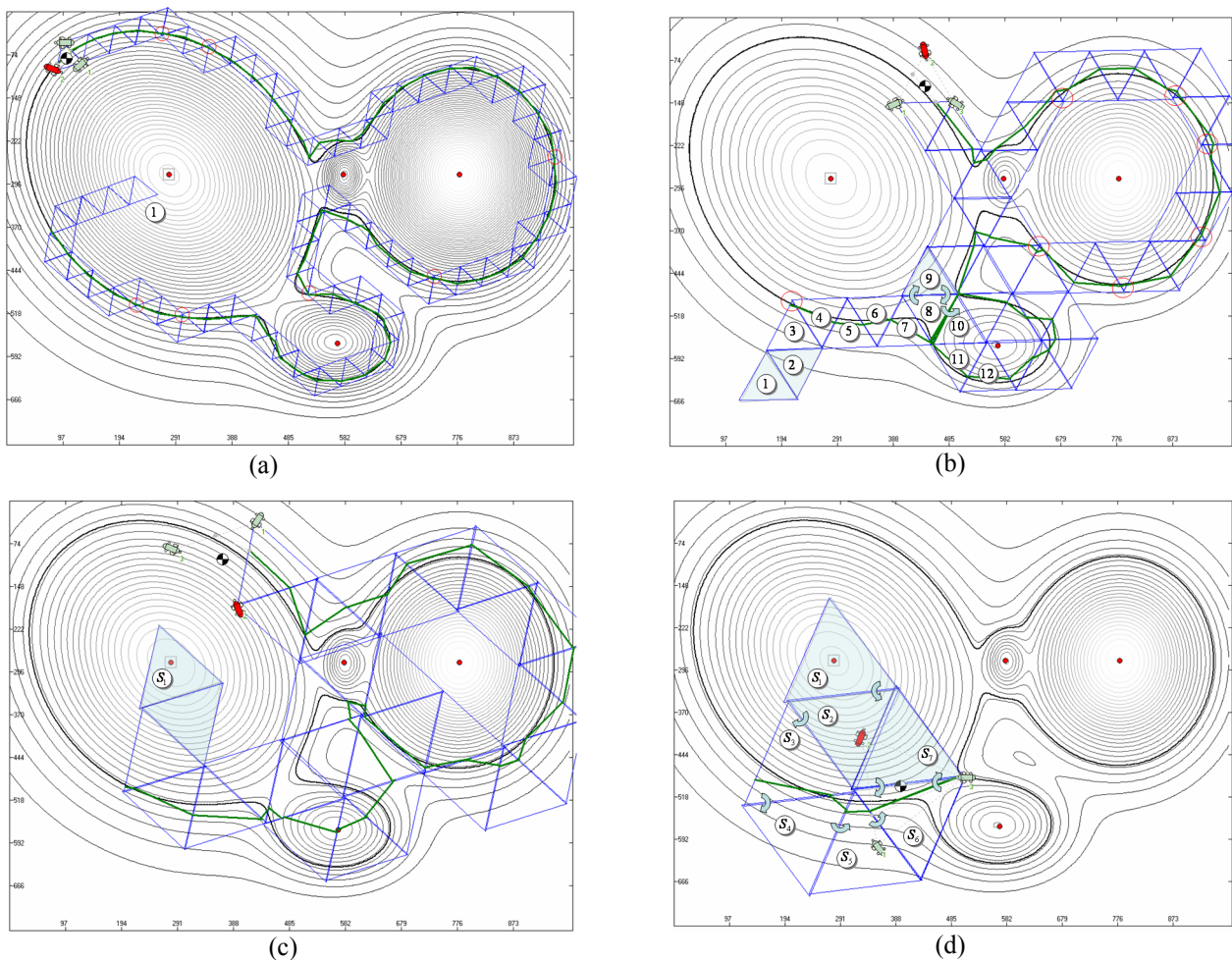
figure 10: Formations of different sizes against an isocline. (a) $L_S = 50$. (b) $L_S = 100$. (c) $L_S = 150$. (d) $L_S = 200$.

not the case, the formation continues traversing the obstacle.

Terrain reconstruction. After the completion of traversal of an isocline, a set of approximations to the isoclines will be available for interpretation by human operators. At this stage, an approximation to an isocline would be a set of disconnected line segments which may not be suitable for analysis. To create smooth curves, we may first define a smooth landscape using the line segments as skeleton, choose a level set of it and then have an *active contour* [14] adapt itself to the level set. Once a set of smooth curves representing isoclines have been thus obtained, we can use the strategy proposed in [6] to partially reconstruct the field using interpolation.

System architecture. Figure 8 shows a hybrid state diagram of the whole operation cycle. Implementing this system on physical robots requires simple coordination and communication between robots. However, the underlying technology is not trivial and involves accurate distance and bearing measurement in aquatic environments.

6. Simulations

Figure 9(a) shows a formation climbing an artificial landscape to reach an isocline surrounding a peak. Figure 9(b) shows a formation traversing an isocline. The arrows indicate the direction of flipping around the pivot while the green lines show the history of linear models after each reflection (polygonal approximation to the isocline). Note that the line segments are not equal in length. The red dots indicate peaks. Figure 10 shows the performance of formations of different sizes in tracking the same isocline. The shaded triangles are those which do not have an intersection with the isocline. Red circles indicate locations where the intersection of the linear model with the triangle is very small. The formation with $L_S = 50$ has done a reasonably well job of tracking. The larger formation ($L_S = 100$) gets into trouble when reaching S_8. S_9 is not on the isoline and flips back unto S_8. Falling outside is due to the fact that the size is too large. Also, the segment $\{w_1, w_2\}$ for S_8 is almost colinear with one of the sides. This goes on for a few steps before, due to errors in simulation, the formation can eventually escape this situation.
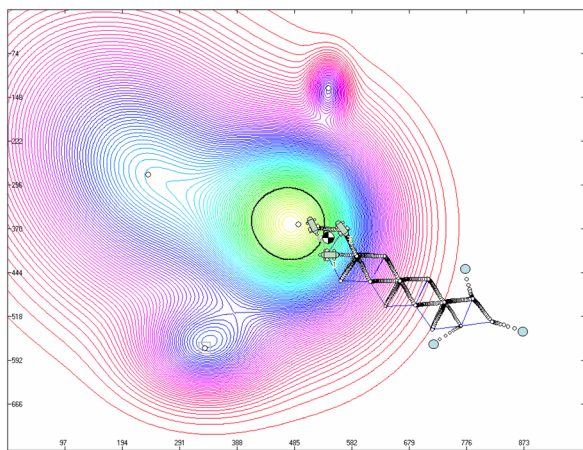
(a)
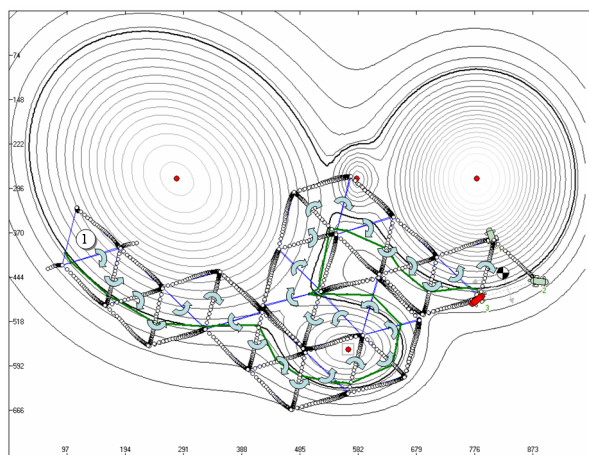
(b)

figure 9: Reaching ((a)) and tracking ((b)).
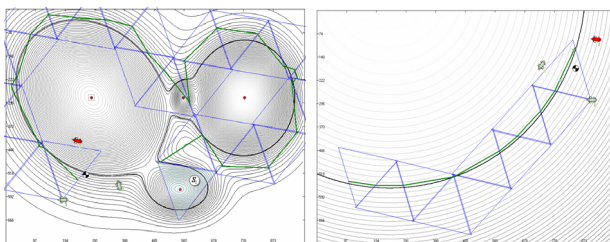
(a)   (b)

figure 11: Large formations. (a) high curvature. (b) Low curvature.

Due to initial conditions, the formation with $L_s = 150$ is able to track the isoline, albeit with deteriorated quality for approximation. Finally, the larger formation in figure 10(d) cannot escape the visious loop without reducing its size. In contrast, figure 11(a) shows the successful traversal of an isocline with high curvature by this formation. Figure 11(b) shows the same formation in an environment with low curvature. These runs emphasize the importance of having an adaptive mechanism for size change and one that maneuvres the formation to a more appropriate posi-

tion with respect to the isocline before deciding on the next action. This will reduce uncertainty and create equal segments.

7. Conclusions and future research

In this paper, we proposed the use of a simplex-based direct optimization strategy for reaching isoclines and tracking them. In this method, the formation traverses a tesselation of the plane. We used the same simple idea behind hill-climbing to traversing those elements of the tesselation that overlap with a desired isocline. Simulations clearly show that successful operation needs a mechanism for location adjustment (just enough to eliminate uncertainties) and size adaptation. We also mentioned that this same method can be used for obstacle avoidance, providing a unified navigation scheme based on reflection only. These, as well as strategies for coordinating groups of formation (dispersal, rendezvous) to cut task completion time, will be dealt with in subsequent publications.

References

[1] J http://users.rsise.anu.edu.au/~serafina/

[2] Kalantar, S., *Field-Coupled Deformable Formations of Autonomous Submersible Robots*, PhD Thesis, The Australian National University, 2006.

[3] Reet, A.V., *Contour Tracking for the REMUS Autonomous Underwater Vehicle*, Master's thesis, Dept. of Mech. Eng., US Naval Postgraduate School, 2005.

[4] Zhang, F., Leonard, N.E., *Generating Contour Plots using Multiple Sensor Platforms*, Proc. IEEE Swarm Intelligence Symp., 2005.

[5] Ogren, P., Fiorelli, E., Leonard, N.E., *Formations with a Mission: Stable Coordination of Vehicle Group Maneuvres*, Proc. 15th Int. Symp. on Math. Theory of Networks and Systems, 2002.

[6] Hormann, K., Spinello, S., Schroder, P., C^1-*Continuous Terrain Reconstruction from Sparse Contours*, 8th Int. Fall Workshop on Vision and Visualization, Munich, Germany, 2003.

[7] Pang, S., Farrell, J.A., Arrieta, R.M., Li, W., *AUV Reactive Planning: Deepest Point*, Proc. of IEEE Oceans Conf., San Diego, USA, 2003.

[8] Byrne, R.H., Eskridge, S.E., Hurtado, J.H., Savage, E.L., *Algorithms and Analysis for Underwater Vehicle Plume Tracing*, SANDIA Report SAND2003-2643, Sandia National Laboratories, 2003.

[9] Ogren, P., Fiorelli, E., Leonard, N.E., *Cooperative Control of Mobile Sensor Networks: Adaptive Gradient Climbing in a Distributed Environment*, IEEE Trans. on Automatic Control, 49(8), 2004.

[10] Kolda, T.G., Lewis, R.M., Torczon, V., *Optimization by Direct Search: New Perspectives on some Classical and Modern Methods*, SIAM Review, 45(3), 2003.

[11] Burian, E., Yoerger, D., Bradley, A., Singh, H., *Gradient Search with Autonomous Underwater Vehicles Using Scalar Measurements*, Proc. of IEEE Symp. on Autonomous Underwater Vehicle Technology, Monterey, CA, USA, 1996.

[12] de Sousa, J.B., Johansson, K.H., Speranzon, A., Silva, J., *A Control Architecture for Multiple Submarines in Coordinated Search Missions*, Proc. of the 16th IFAC World Congress, 2005.

[13] Cleveland, W.S., *Visualizing Data*, Hobart Prtess, Summit, New Jersey, USA, 1992.

[14] Kass, M., Witkin, A., Terzopoulos, D., *Snakes: Active Contour Models*, Intl. Journal of Computer Vision, 1(14), 1987.